# *Associative Behavior-Based abundance Index (ABBI) for Yellowfin tuna (Thunnus albacares) in the Western Indian Ocean*

Yannick Baidai*[1], Amaël Dupaix[3], Laurent Dagorn[2], Jean-Louis Deneubourg[3], Antoine Duparc[2], Taha Imzilen[2] and Manuela Capello[2]

[1] African Marine Expertises, 04 BP 2991 Abidjan 04, Côte d'Ivoire,

[2] MARBEC, Univ. Montpellier, CNRS, Ifremer, IRD, Sète, France,

[3] Unit of Social Ecology, Université Libre de Bruxelles (ULB), Bruxelles, Belgium.

## Abstract

The traditional CPUE abundance indices used for stock assessment currently face multiple challenges due to the use of novel technologies, changes in fishing strategies and contraction of fishing effort. Since several years, the program of work of the IOTC WPTT emphasizes the need for alternative indices of abundance for tropical tuna, including abundance estimates obtained from acoustic data of echosounder buoys. This study presents the Associative Behavior-Based abundance Index (ABBI) for yellowfin tuna *(Thunnus albacares)* in the Western Indian Ocean. The ABBI builds on knowledge of the associative dynamics of tuna within arrays of floating objects (FOBs) obtained from non-conventional data (acoustic tagging and echosounder buoys) and conventional data (species composition and size of FOB aggregations obtained from logbook and port sampling data), to provide an alternative index of abundance to support stock assessment.

## Introduction

The production of alternative indices of tuna abundance has been identified as a priority by the Indian Ocean Tuna Commission (IOTC 2023). This is particularly important for yellowfin tuna, which is currently overfished and subject to overfishing (IOTC 2023). Standardized longline CPUEs provide the primary relative abundance index for the stock assessment of yellowfin tuna. However, contraction of effort over time and changes in fishing strategies within this fishery pose challenges for accurately assessing abundance indices through longline fisheries data (IOTC 2021). Another important fishery that offers large spatial coverage and long term time series for catch and effort data is the industrial purse seine tuna fishery that operates in the Western Indian Ocean. However, the main challenges in deriving reliable CPUE indices from tropical tuna purse-seine fisheries data consist in accounting for the frequent integration of new technologies on-board the industrial purse seine vessels and for the continuous evolution of their fishing strategies, which make effort estimates difficult to conduct (Torres-Irineo et al. 2014, Fonteneau et al 2013). The widespread use of drifting fish aggregating devices (DFADs), which has expanded even further since the introduction of TAC for yellowfin tuna, further complexifies the derivation of the CPUE from purse seine catches. The effort unit that was historically used in the past to produce CPUE indices from purse-seine catch data was the number of search days, i.e., the number of days required to find and fish free swimming schools (i.e., tuna schools non associated with floating objects). With the introduction of DFADs and their related technology (GPS and echosounder buoys) the number of search days clearly became obsolete, since fishing on DFADs is highly driven by the remote reception of DFAD positions and the acoustic data collected by echosounder buoys, used by skippers as a proxy of the tuna associated biomasses. Recently, CPUE indices based on DFAD catches have been developed, considering the catch-per-set at DFADs as an index of abundance. These indices make the implicit assumption that the size of tuna aggregations is proportional to the tuna abundance. Potential hyperstability issues related to the use of such indices have been recently debated (IOTC 2023).

Tropical tuna naturally associates with floating objects (FOBs) found at the surface of the open ocean. The type and nature of the FOBs does not appear to play a major role in the association dynamics. In the literature, the term "FOBs" includes natural floating objects (NLOGs), DFADs or other FAD types (such as anchored FADs), or marine debris of other anthropogenic origin (e.g., macro-plastics). The associative dynamics of the three main tropical tuna species (yellowfin, skipjack and bigeye tuna) at FOBs has been well characterized, both at the level of the individuals, through acoustic tagging experiments (e.g. Robert et al. 2012, Matzumoto et al. 2014, Rodriguez-Tress et al. 2017, Pérez et al. 2020, Govinden et al. 2021), and at the level of the tuna aggregations, through echosounder buoys data (Baidai et al 2020). Acoustically-tagged tuna individuals tagged within arrays of instrumented anchored FADs appear to alternate association periods at FADs (the so-called CRTs, continuous residence times) and periods spent "unassociated", i.e., far away from the FOBs (the so-called, CAT, continuous absence times). Similarly, DFADs continuously monitored through echosounder buoys have been shown to alternate periods where they are occupied by tuna aggregations and periods where they are empty (Baidai et al 2020).

This study presents the *Associative Behavior-Based abundance Index (ABBI*), an index of tuna abundance that that builds on this knowledge of the tuna association dynamics at FOBs obtained from non-conventional data. The ABBI index, derived for the main yellowfin tuna size class that associates with FOBs (weight < 10 Kg) in the Western Indian Ocean, can offer an alternative method of estimating tuna abundance compared to more conventional CPUE-based abundance indices.

**The ABBI theoretical framework**

The associative behavior of tropical tuna species implies that, at any given time *t*, the overall abundance (*N(t)*) in an area with *p* FOBs, results from the sum of the abundances of their associated component ($X_a(t)$) located nearby FOBs and unassociated ($X_u(t)$) component, located away from FOBs (*i.e.*, free-swimming tuna schools).

$$N(t) = X_a(t) + X_u(t) \qquad \text{[eqn. 1]}$$

Within a given study region and time period, the biomass of the associated component of the tuna population ($\widehat{X_a}$) can be estimated as follows:

$$\widehat{X_a} = \widehat{m}\hat{f}\hat{p} \qquad \text{[eqn. 2]}$$

Where $\widehat{m}$ is the estimated average tuna biomass associated with a FOB, $\hat{f}$ represents the estimated proportion of FOBs occupied by tuna and $\hat{p}$ the estimated number of FOBs in the region/period of interest. Previous studies (Capello et al. 2016) demonstrated that the ratio between the associated component and the total population ($\widehat{N}$) can be derived by measuring the uninterrupted period of time that tunas spend either associated with, or unassociated from a FOB, *i.e.*, the average continuous residence time (CRT) and the average continuous absence time (CAT):

$$\frac{\widehat{X_a}}{\widehat{N}} = \frac{CRT}{CRT + CAT} \qquad \text{[eqn. 3]}$$

Combining equations 1-3, the total population can then be estimated as follows:

$$\widehat{N} = \widehat{m}\hat{f}\hat{p}\left(1 + \frac{CAT}{CRT}\right) \qquad \text{[eqn. 4]}$$

As the associative dynamics of tuna are dependent on species and size (e.g. Robert et al. 2012, Matzumoto et al. 2014, Rodriguez-Tress et al. 2017, Pérez et al. 2020, Govinden et al. 2021), equation 4 is applicable on a species and size classes basis, where the same associative behavior with FOBs is expected. Furthermore, considering the above equations, the biomass of the unassociated component of the tuna population can be estimated as follows:

$$\widehat{X_u} = \frac{CAT}{CRT}\widehat{m}\hat{f}\hat{p} \qquad \text{[eqn. 5]}$$

**Derivation of ABBI for yellowfin tuna in the Indian ocean**

Estimating yellowfin tuna abundance from the ABBI framework as provided by equation 4 requires a set of input data which is currently available in the Western Indian ocean. The abundance estimates were conducted between 2013 and 2021, using a spatio-temporal stratification of 10°×10° and quarter-year (Fig. 1). ABBI indices of abundance were estimated within each stratum for each species and population components (estimated total population (eqn.4); estimated size of the associated component (eqn. 2); estimated size of the unassociated population (eqn.5)). For yellowfin tuna, only the component of the population related to small individuals (weight under 10 kg) was considered. This corresponds to the main size category caught at FOBs and for which data on residence and absence times have been measured (Govinden et al 2021).

ABBI abundance indices over the entire study area were estimated from the average of the quarterly ABBI indices obtained over the available strata, resulting in a final index representing the average abundance per 10°×10° square and quarter. Finally, ABBI relative abundance indices were provided using the ABBI abundance indices of the first available quarter of 2013 (*i.e.* the first quarter in which the input dataset for the implementation of ABBI was available) as reference.

**Estimated number of floating objects ($\widehat{p}$)**

Drifting FOBs considered in this study consist of two main categories: DFADs and “other objects”. The DFAD category contains FOBs specifically designed and deployed by fishers to encourage tuna aggregations, while the “other objects” category includes natural drifting objects (*e.g.* branches or logs) and anthropogenic debris (artificial objects resulting from human activities related or not to fishing). Due to the availability of DFAD location data changing over time, the estimation of the total number of FOBs within each time-area unit followed two different approaches.

From 2013 to 2019, time series of the total number of FOBs were constructed from the echosounder buoys database hosted by the “Observatoire des Ecosystèmes Pélagiques Tropicaux Exploités” (Ob7/IRD/MARBEC). The dataset consists of position data collected by the “Marine Instruments” echosounder buoys deployed on DFADs by the French fleet in the Indian Ocean. First, the average number of buoys was calculated from this database, for each spatio-temporal stratum (10°/quarter). Then, total numbers of FOBs (DFADs and "other objects") in the different strata were estimated by applying multiplication factors taking into account the number of DFADs belonging to other purse seine fleets, as well as the “other objects” category.

From 2020 to 2021, the estimation of FOBs number have benefitted from the recent availability of echosounder buoys data from tuna purse-seine vessels provided by the IOTC Secretariat [55]. This dataset consists of the monthly average of the number of operational buoys (i.e., echosounder buoys that remotely transmit their position) for each 1°×1° cell of the Indian Ocean. The total number of FOBs in the different strata was then estimated by aggregating the data according to the level considered in the spatio-temporal strata of the study, and applying a raising factor to account for the number of "other objects". Further details of the calculation can be find in Supplementary Information S1. Figure 2 provides estimates of the number of FOBs in the study area.

### Estimated FOB-associated tuna biomass ($\hat{m}$)

The average biomasses of small yellowfin tuna (size category under 10 kg) around a FOB were derived from purse seine catch-per-set data reported in the vessel logbooks of the French fleet (Table 1). In order to improve the accuracy of the estimated catches, FOB-associated catches-per-set reported in vessel logbooks were corrected using a dedicated procedure referred to as levels 1 and 2 of the T3 processing (see e.g. Duparc et al. 2020). Level 1 adjusts the catch-per-set values declared in vessel logbooks using landing notes, to improve the accuracy of catch estimates provided by skippers. Level 2 estimates the species and size compositions of FOB sets based on port sampling data.

Since landing notes were available for all fishing trips, Level 1 was applied to correct the reported catch-per-set of all FOB sets recorded in vessel logbook data. Level 2, on the other hand, was applied only to the FOB sets conducted during the fishing trips that were sampled at landing. These FOB sets are referred to as “sampled FOB sets”.

Species compositions (i.e., percentages of catches by species and size category in the sampled FOB sets) were averaged by stratum, with a minimum threshold of 20 available sampled FOB sets per strata. Where species composition values were missing for a given stratum, they were generated using their corresponding estimated marginal means (*aka* least-squares means), following a procedure described in the Supplementary Information S2.

Finally, the average biomasses of small yellowfin tuna (size category under 10 kg) associated with a FOB ($\hat{m}$) were calculated for each stratum by multiplying the average catch-per-set of all FOBs (including both sampled and not-sampled sets, all adjusted through the level 1 of the T3 processing) by the average species composition. Only the strata with at least 20 FOB sets (including both sampled and not-sampled sets) were retained for the estimation of $\hat{m}$ and the derivation of the ABBI index. The catch and species composition data provided by the Ob7 were collected under the Data Collection Framework (Reg. 2017/1004 and 2016/1251) funded by IRD and the European Union. Fig. 3 shows the time series of the FOB-associated biomasses ($\hat{m}$) obtained for yellowfin tuna, across the various spatial strata considered.

**Estimated proportion of FOBs occupied by tunas ($\hat{f}$)**

The proportions of FOBs occupied by tuna were estimated from the acoustic data collected by the “Marine Instruments – M3I” satellite –linked echosounder buoys deployed on FOBs monitored by the French tuna purse seine fleet in the western Indian Ocean (also available from the OB7 hosted echosounder buoys database). This model of buoy has an integrated echosounder device (frequency 50 kHz, power 500 W, beam angle of 36°), which provides acoustic information on the biomass associated with the FOB, with a detection threshold of one tonne [50]. This detection threshold was considered satisfactory as it ensured consistency between the datasets of estimated FOB occupancy rate ($\hat{f}$) and associated biomass ($\hat{m}$) estimated from catch data because fishing operations are seldom carried out on FOBs with less than one tonne of associated tuna biomass (approximately 0.5% of the fishing sets performed by French tuna purse seine fleet in the Indian Ocean). Processing acoustic data from buoys using a machine learning algorithm, whose accuracy has been demonstrated (85%) in the Indian Ocean (Baidai et al. 2020), allowed for geolocated times series of tuna presence/absence data under FOBs. Then, the initial segments immediately following the deployment of the FOBs, consisting of tuna absence data, were excluded from the analysis as they reflect the FAD colonization period (Baidai et al 2020).

Daily presence/absence data were used to derive the estimated proportion of FOBs with tuna associated ($\hat{f}$). This was expressed as the number of FOBs (equipped by an M3I buoy) occupied by tunas, divided by the total number of M3I buoys available in the database, calculated on a daily basis. A threshold of at least 30 available M3I buoys per day was considered when calculating the daily proportion of FOBs occupied by tuna across the spatial strata. Table 1 provides the average daily numbers of available M3I buoys over the full study area for each quarter.

The buoy technology remains limited in its ability to discriminate between the various tuna species (Baidai et al 2020). Nevertheless, this limitation can be overcome to achieve finer grained details on FOB occupancy at a species-level. This is achieved by combining the estimated fraction of FOBs occupied by tunas ($\hat{f}$) with the rate of occurrence of each species in FOB aggregations obtained from FOB catches and sampling data, according to the following equation:

$$\widehat{f_i} = \hat{f} . \widehat{\eta_i} \qquad \text{[eqn. 6]}$$

where $\widehat{f_i}$ denotes for the estimated proportion of FOBs occupied by the tuna species $i$, and $\widehat{\eta_i}$ represents the ratio of the number of FOB associated sets that resulted in a catch greater than or equal to 1 ton of the species in question, to the total number of FOB sets. This ratio was estimated on a quarterly basis, within each 10°x10° spatial stratum, using data from port sampling programs. A minimum number of 20 available sampled fishing sets per strata was considered for the ratio calculation. Missing occurrence values for a given stratum were estimated from a binomial model using year, quarter and spatial strata as predictors (Supplementary Information S3). The time series of $\hat{f}$ for yellowfin tuna are presented in Fig. 4.

**Continuous residence time (CRT)**

The CRT values were provided by the acoustic tagging experiments carried out around DFADs in the study area by Govinden et *al.* (2021), whose estimates of the CRTs of small yellowfin (62 fork length on average) around a DFAD were 6.7 ± 7.8 days.

**Continuous absence time (CAT)**

At the time of the study, only CRTs were measured for the three species on DFADs. However, acoustic tagging experiments conducted in arrays of anchored Fish Aggregating Devices (AFADs) showed that CATs decrease for decreasing distances among AFADs, due to an increased AFAD encounter rate by tuna at higher AFAD densities (Pérez et al. 2020). Based on these findings, the following Ansatz relating the average CAT to the number of FOBs ($\hat{p}$) was used:

$$CAT = \frac{1}{\phi\hat{p}} \qquad \text{[eqn. 7]}$$

where $\phi$ is a parameter that depends on the probability of associating to one of the estimated $\hat{p}$ FOBs. To assess the sensitivity of the ABBI to this parameter, ranges of $\phi$ in the range [1e-05, 6e-05] were considered. Substituting these values in Eq.7 produces average CATs ranging between 10 and 60 days for an average density of FOBs of ~1700 FOBs per 10°×10° square in the study region), consistent with the ranges of CATs found from acoustic tagging studies (Pérez et al.2020, Rodriguez Tress et al. 2017, Robert et al. 2013) (Fig. 5).

**ABBI index estimated for yellowfin tuna**

Figures 6, 7 and 8 provide the estimated associated, free and total population of yellowfin tuna for each 10° stratum in the study region, using Eqs. 2, 5 and 4, respectively. The estimated free and total population show a strong dependence on the φ parameter used to estimate CATs (Eqn.7).

Finally, Figure 9 provides the time ABBI for the whole study region. The total yellowfin tuna abundance shows high sensitivity to the φ parameter. However, the relative abundance index is more robust with respect to changes in φ and demonstrates steady levels of abundance from the last quarter of 2018 onwards.

## Figures

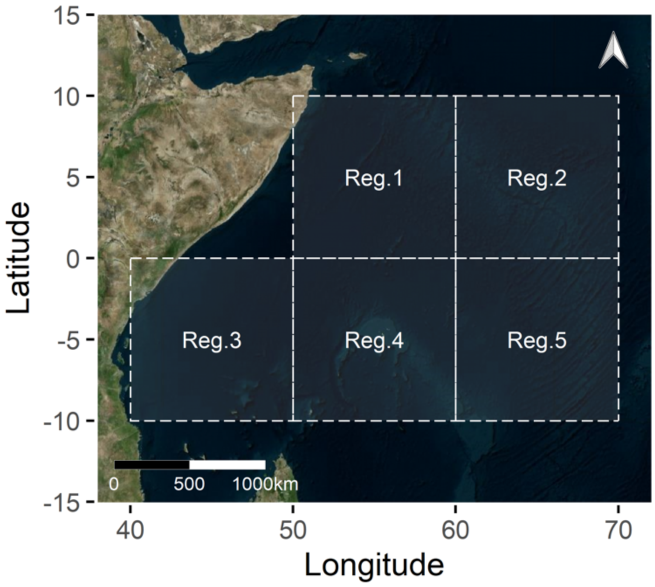


**Figure 1:** Spatial stratification of the study area. The abundance estimates were conducted individually in each of the five regions identified by the abbreviation “Reg.”. Then, an average abundance index for the entire study area was derived.

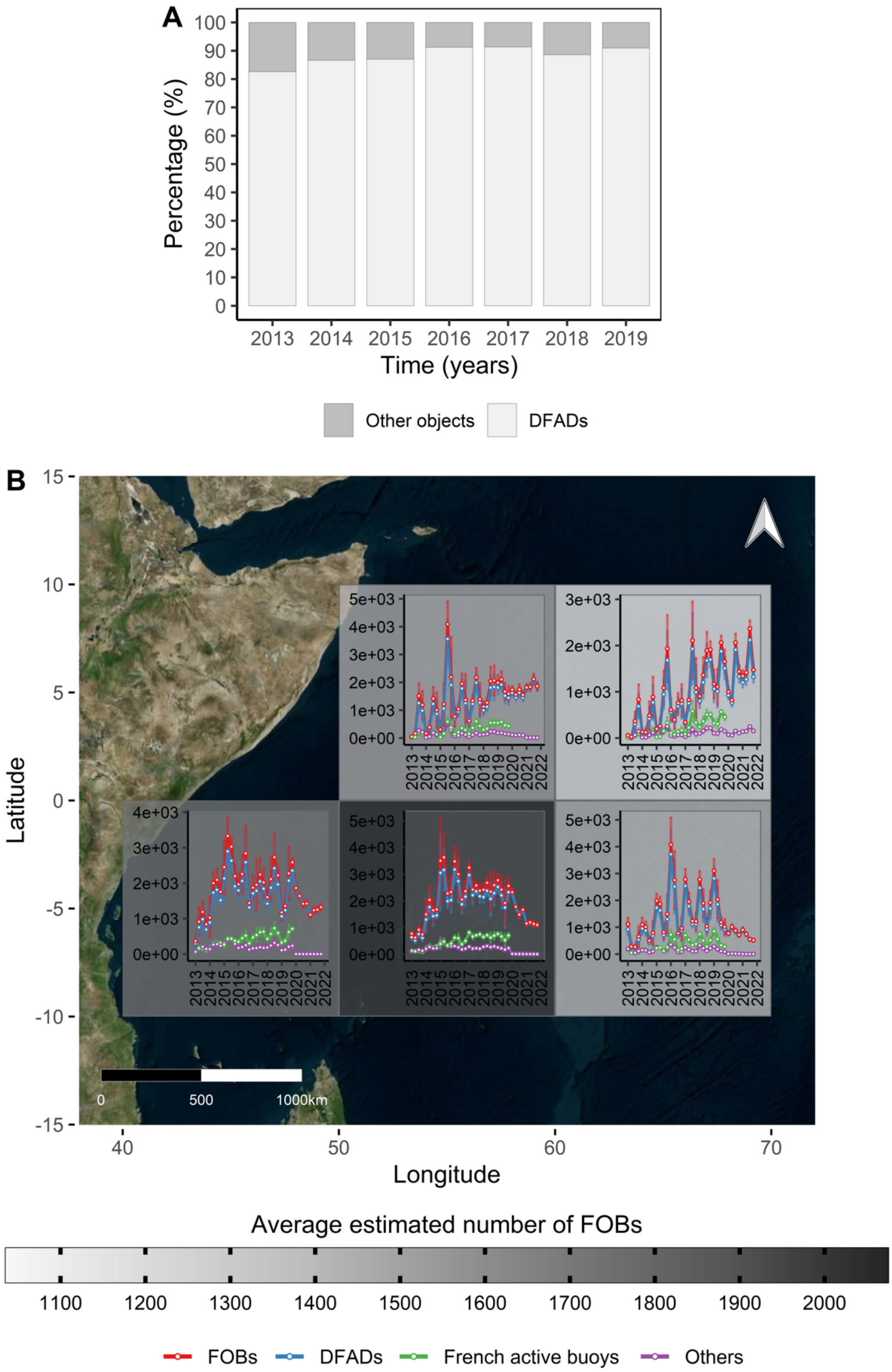


**Figure 2:** Estimates of the number of floating objects in the study area. (A) Percentage of drifting fish aggregating devices (DFADs) and other types of natural and artificial objects (Other objects) reported by observers on board French tuna purse-seiners. (B) Quarterly averages of the daily number of active buoys in the French fleet, the estimated numbers of drifting fish aggregating devices (DFADs), the other objects (Others), and the estimated total number of floating objects (FOBs = DFADs + Others) by 10° × 10° spatial strata in the western Indian Ocean. The background colors indicate the average number of FOBs calculated from 2013 to 2019 in each stratum.

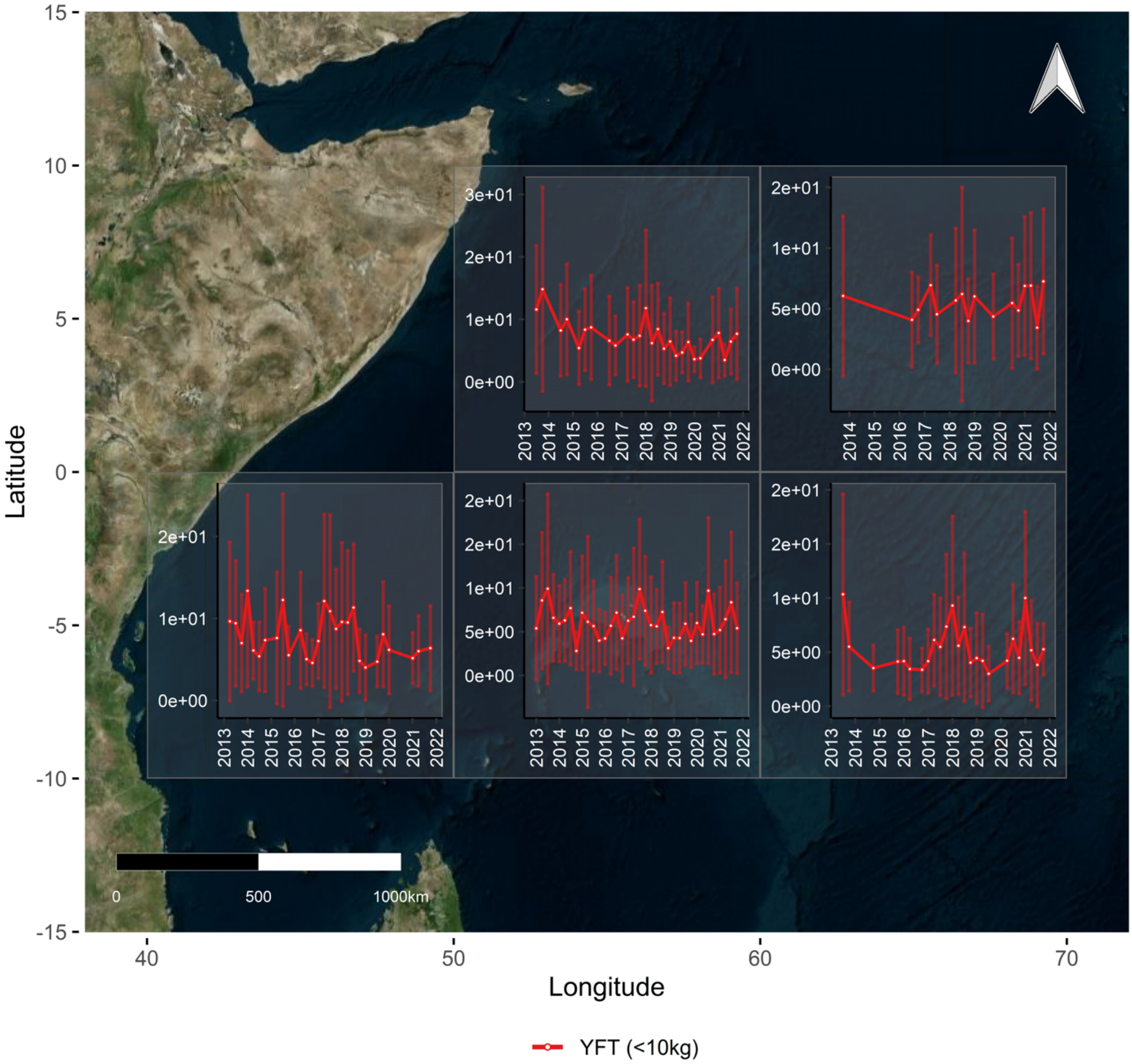


**Figure 3 |** Quarterly averages of FOB-associated biomasses (in tonnes) of yellowfin tuna under 10kg (YFT <10kg) per FOB set by 10° × 10° spatial strata in the western Indian Ocean.

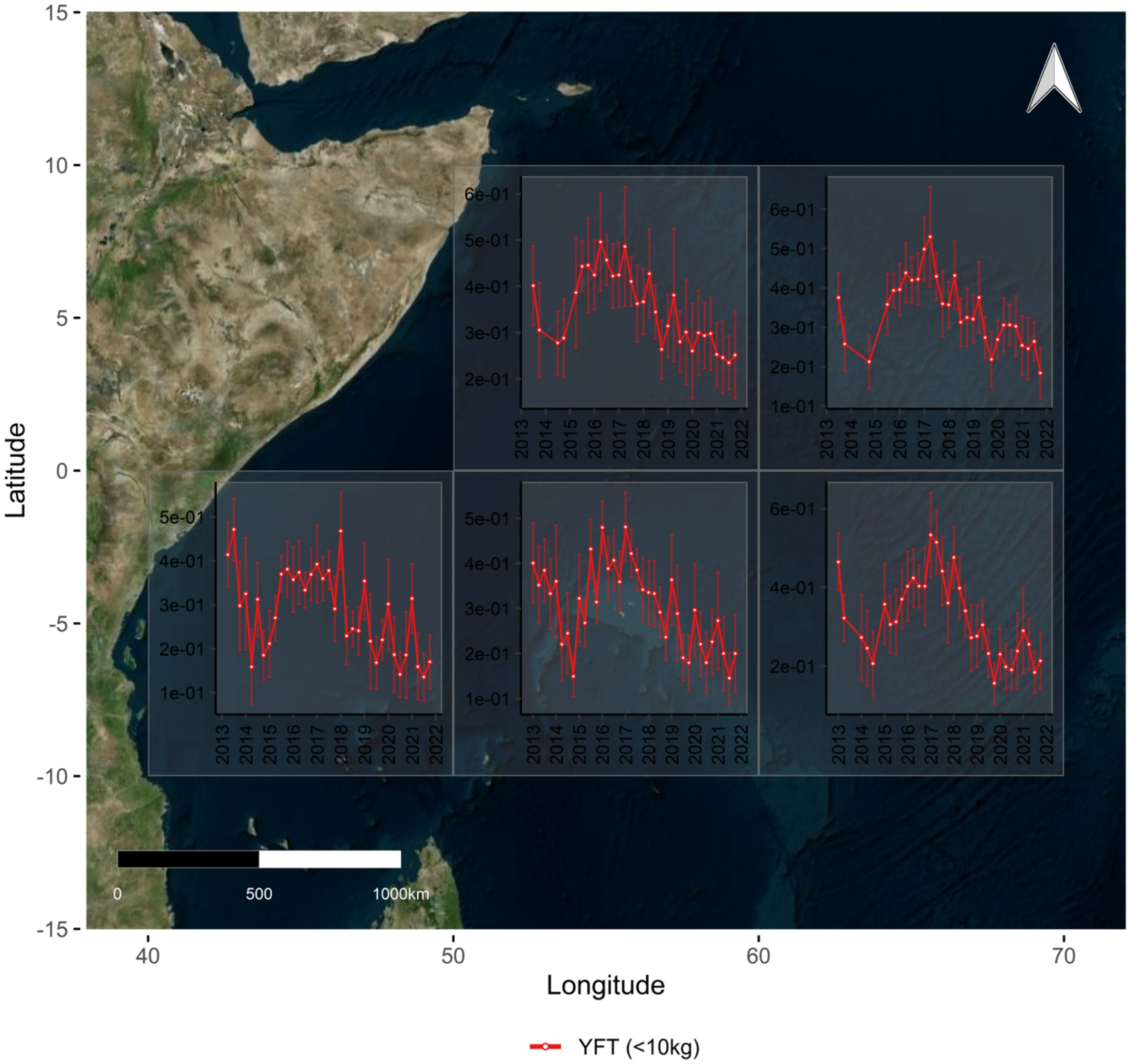


**Figure 4 |** Quarterly averages of the daily proportion of inhabited FOBs for yellowfin tuna under 10 kg, by 10°×10° spatial strata in the western Indian Ocean from 2013 to 2021 in each spatial stratum.

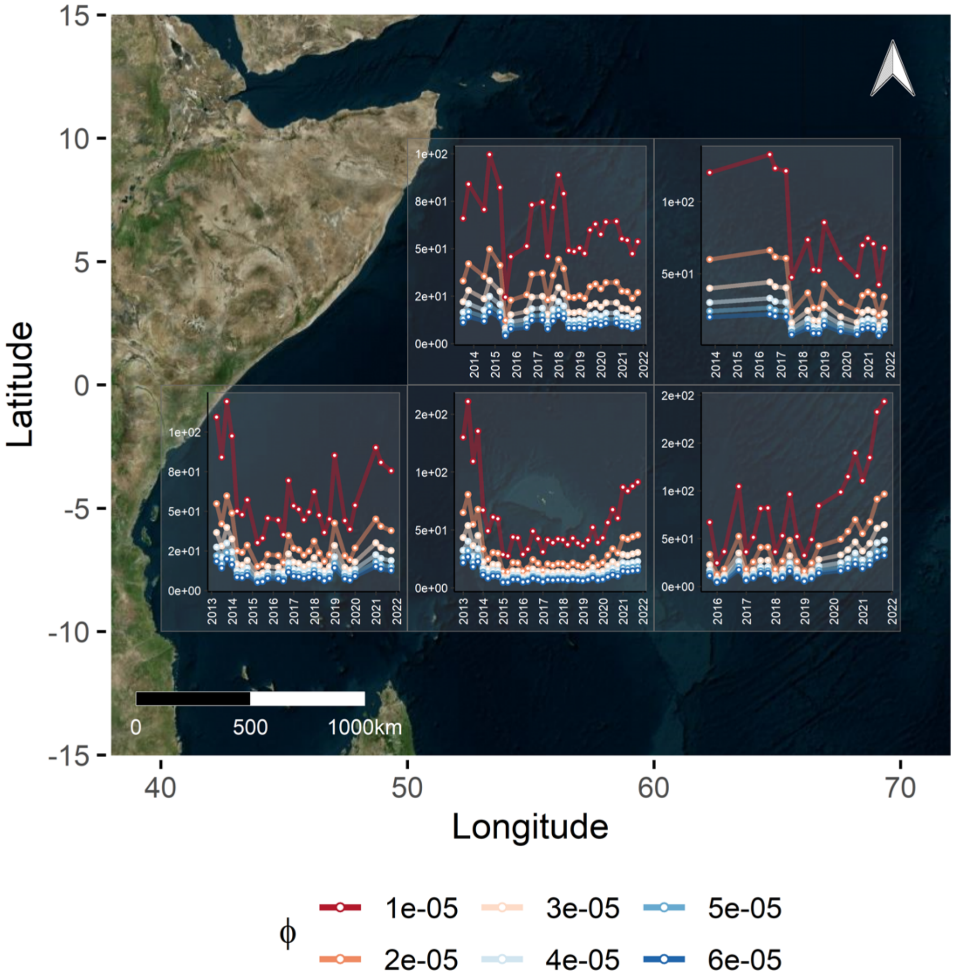


**Figure 5 |** Quarterly averages of estimated tuna CAT under different values of $\phi$.

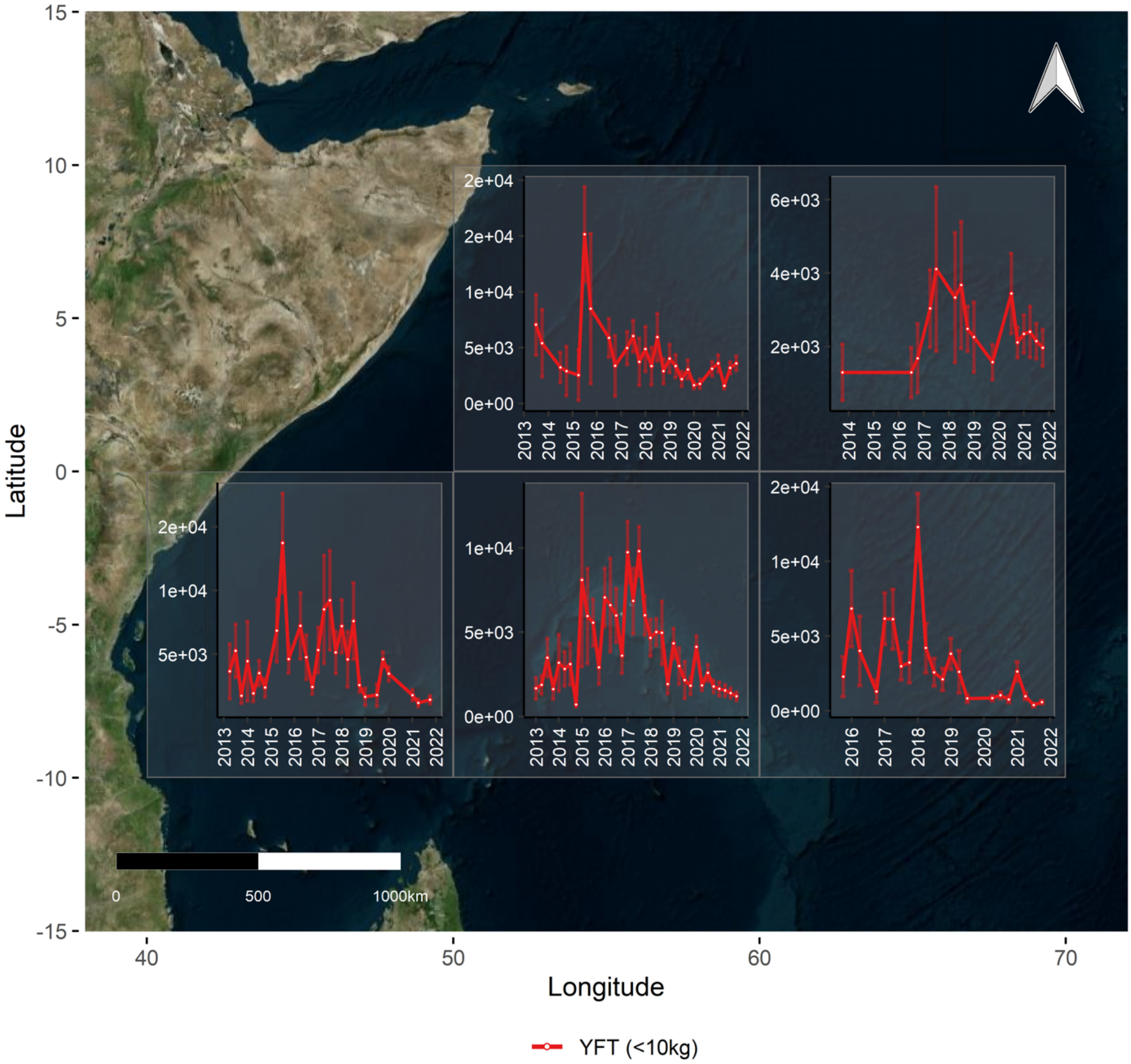


**Figure 6 |** Quarterly estimates (in tonnes) of the average associated component of yellowfin tuna (under 10 kg) stock, by 10°×10° spatial strata in the western Indian Ocean though the Associative Behavior Based abundance Index (ABBI) framework.

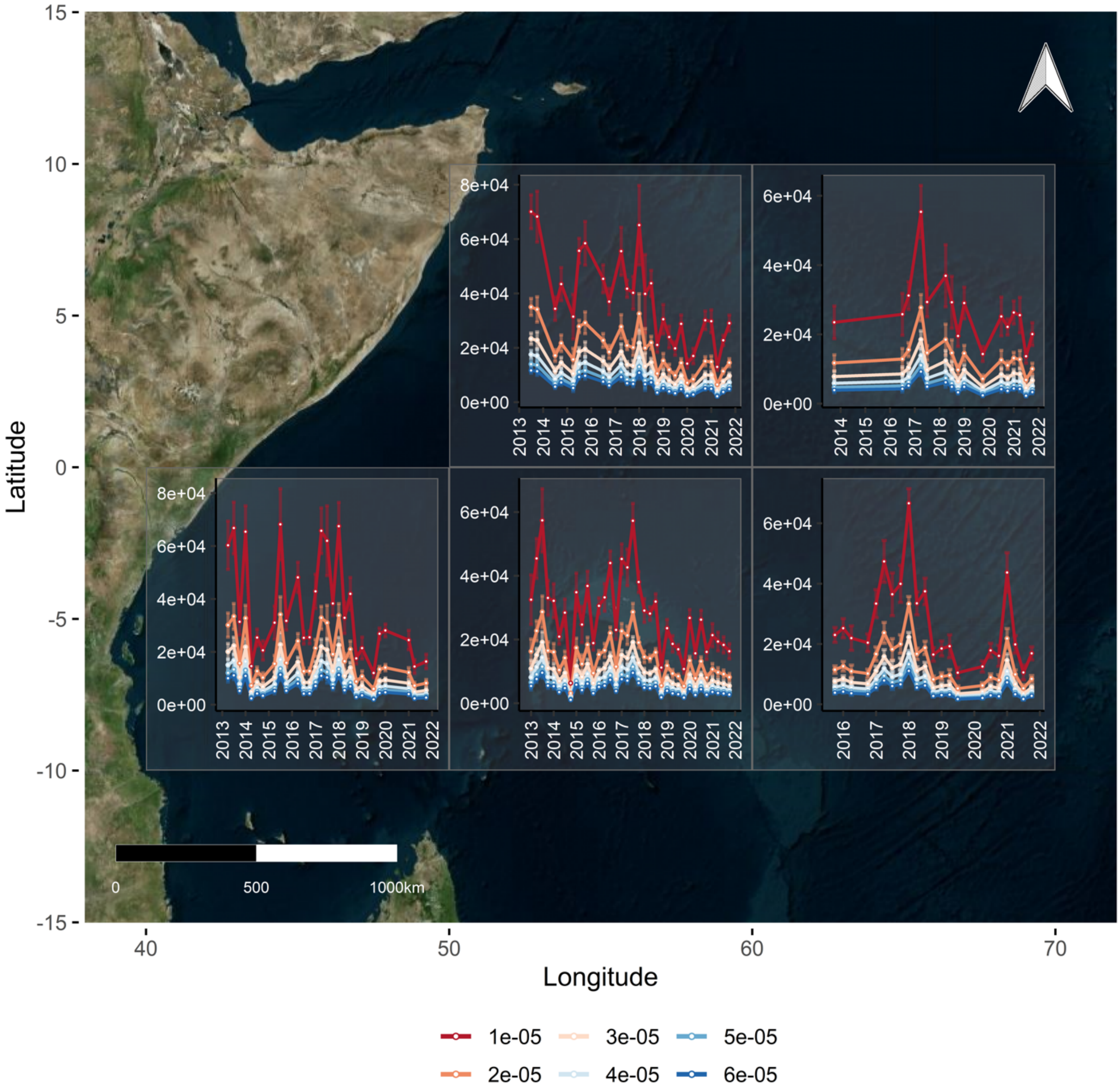


**Figure 7 |** Quarterly estimates (in tonnes) of the average unassociated (free) component of yellowfin tuna (under 10 kg) stock, by 10°×10° spatial strata in the western Indian Ocean though the Associative Behavior Based abundance Index (ABBI) framework. The legend corresponds to different values of the $\phi$ parameter used in the derivation of CATs (Eq. 7).

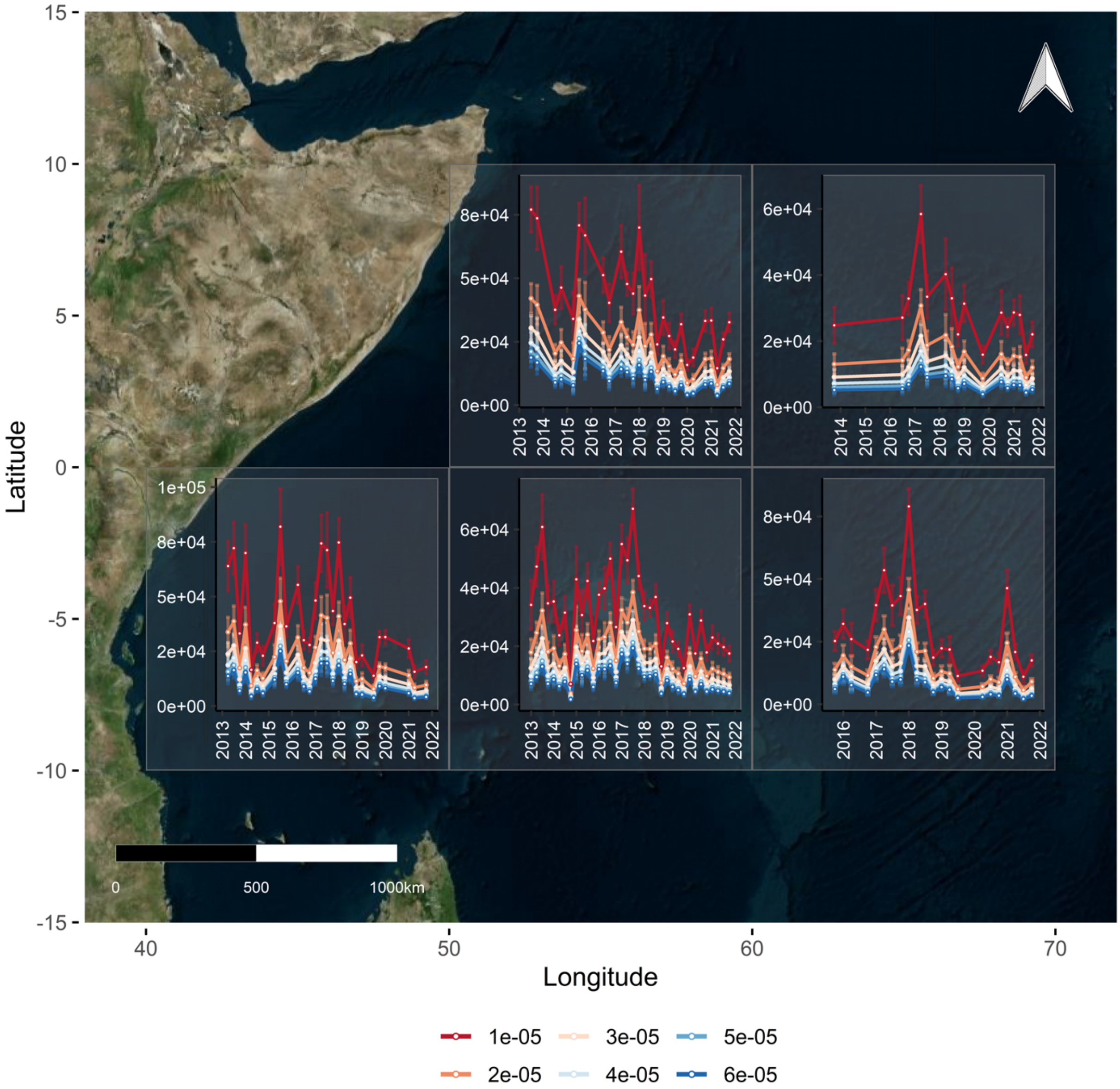


**Figure 8 |** Quarterly estimates of the Associative Behavior Based abundance Index (ABBI) by 10°×10° spatial strata in the western Indian Ocean *for* yellowfin tuna under 10 kg. The legend corresponds to different values of the $\phi$ parameter used in the derivation of CATs (Eq. 7).

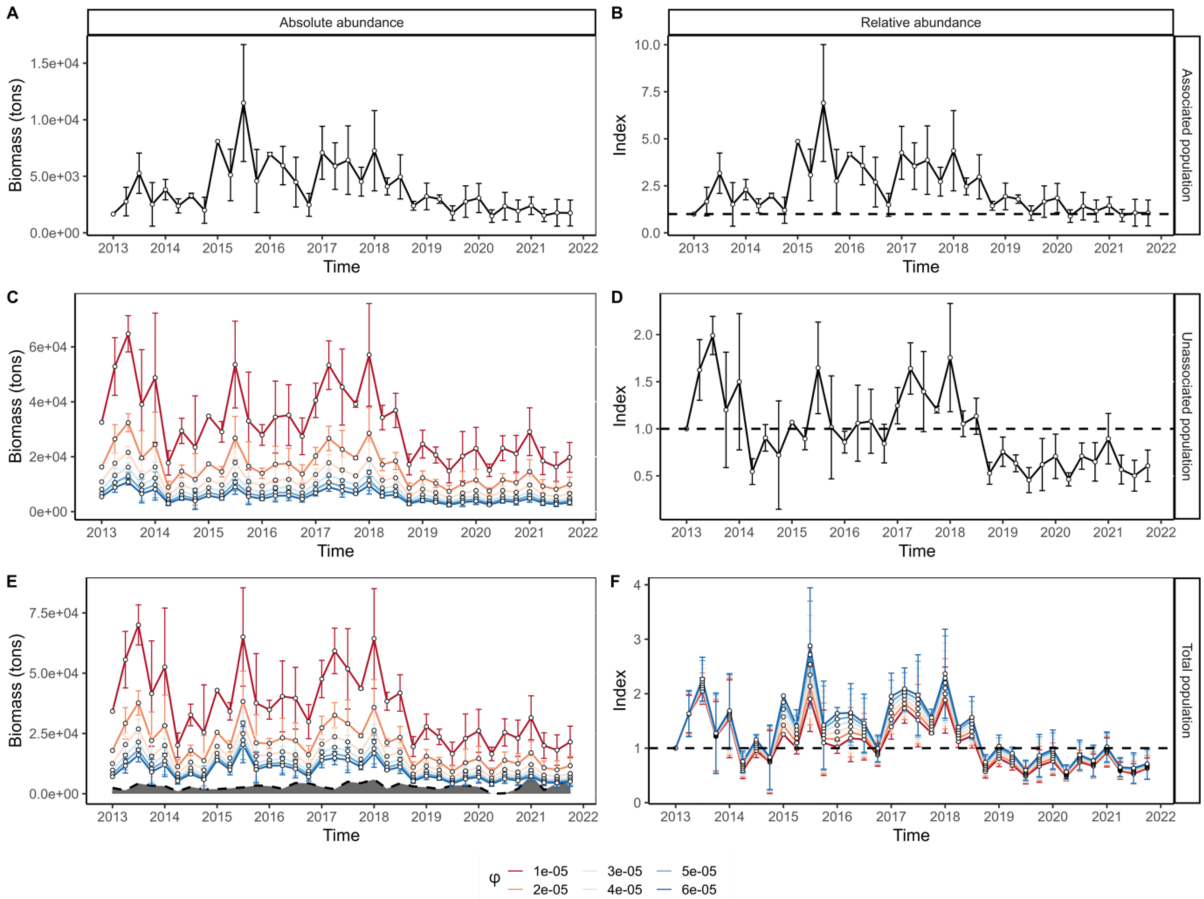


**Figure 9 Absolute and relative indices of abundance of yellowfin tuna (<10Kg) in the Western Indian Ocean.** Estimates of the average associated (A, B), unassociated (free) (C,D) and total biomass of yellowfin tuna (<10 kg) obtained from the ABBI framework in the western Indian Ocean are shown under different values of φ. In the left column. Estimates of each component are obtained considering the averages ((± SE)) over the five 10° x 10° regions of Fig. 6-7-8. Shaded areas in panel (E) correspond to average catches per 10° × 10° square of all the fishing gears targeting yellowfin tuna under 10kg in the same region. In the right column, relative abundance indices for the associated (B), unassociated (free) (D) and total biomass (F) of yellowfin tuna (<10 kg) are obtained considering the value of the first quarter of 2013 as a reference.

# Tables

**Table 1 |** Number of fishing sets on FOBs and buoys used in this study. The "FOB sets" column indicates the total number of fishing sets on floating objects (FOBs) from the logbook data corrected with the T3 process. The "sampled FOB sets" column indicates the number of sampled fishing sets used to estimate the species compositions and occurrences in associated FOB aggregations. "M3I buoy count" and "Total buoy count" represent the daily average number of French M3I buoys and total number of French buoys in the study area by quarter.

| Year | Quarter | FOB sets | Sampled FOB sets | M3I Buoy Count | Total buoy count |
|---|---|---|---|---|---|
| 2013 | Q1 | 171 | 49 | 329 | 333 |
| 2013 | Q2 | 247 | 88 | 349 | 363 |
| 2013 | Q3 | 406 | 112 | 496 | 550 |
| 2013 | Q4 | 505 | 155 | 377 | 509 |
| 2014 | Q1 | 321 | 78 | 328 | 578 |
| 2014 | Q2 | 229 | 54 | 451 | 831 |
| 2014 | Q3 | 472 | 130 | 517 | 927 |
| 2014 | Q4 | 405 | 85 | 666 | 1102 |
| 2015 | Q1 | 139 | 19 | 633 | 927 |
| 2015 | Q2 | 154 | 16 | 1000 | 1338 |
| 2015 | Q3 | 360 | 70 | 1335 | 1620 |
| 2015 | Q4 | 476 | 91 | 1498 | 1738 |
| 2016 | Q1 | 334 | 67 | 1718 | 1941 |
| 2016 | Q2 | 279 | 34 | 1710 | 1876 |
| 2016 | Q3 | 531 | 116 | 1414 | 1541 |
| 2016 | Q4 | 507 | 104 | 1376 | 1468 |
| 2017 | Q1 | 283 | 32 | 2069 | 2223 |
| 2017 | Q2 | 402 | 93 | 1717 | 2324 |
| 2017 | Q3 | 529 | 132 | 2022 | 2841 |
| 2017 | Q4 | 424 | 130 | 1925 | 2528 |
| 2018 | Q1 | 547 | 143 | 1911 | 2366 |
| 2018 | Q2 | 427 | 150 | 2004 | 2494 |
| 2018 | Q3 | 539 | 200 | 2064 | 2690 |
| 2018 | Q4 | 506 | 193 | 2184 | 2866 |
| 2019 | Q1 | 426 | 138 | 1980 | 2807 |
| 2019 | Q2 | 217 | 45 | 1780 | 2485 |
| 2019 | Q3 | 428 | 97 | 1783 | 2507 |
| 2019 | Q4 | 589 | 165 | 1722 | 2589 |
| 2020 | Q1 | 594 | 143 | 1508 | 2447 |
| 2020 | Q4 | 444 | 36 | 903 | 1630 |
| 2021 | Q1 | 359 | 65 | 758 | 1411 |
| 2021 | Q2 | 442 | 139 | 686 | 1571 |
| 2021 | Q3 | 430 | 111 | 775 | 1854 |
| 2021 | Q4 | 519 | 44 | 517 | 1421 |

## References


IOTC. 2023 Report of the 25 th Session of the IOTC Working Party on Tropical Tunas San Sebastian, Spain, 30 October - 4 November 2023.

IOTC. 2021. Report of the 23 rd Session of the IOTC Working Party on Tropical Tunas. Virtual Meeting, 25 – 30 October 2021.

Torres-Irineo E, Gaertner D, Chassot E, Dreyfus-León M. 2014 Changes in fishing power and fishing strategies driven by new technologies: The case of tropical tuna purse seiners in the eastern Atlantic Ocean. *Fish. Res.* **155**, 10-19. (doi:10.1016/j.fishres.2014.02.017)

Fonteneau A, Chassot E, Bodin N. 2013 Global spatio-temporal patterns in tropical tuna purse seine fisheries on drifting fish aggregating devices (DFADs): Taking a historical perspective to inform current challenges. *Aquat. Living Resour.* **26**, 37-48. (doi:10.1051/alr/2013046).

Baidai Y, Dagorn L, Amande MJ, Gaertner D, Capello M. 2020 Tuna aggregation dynamics at Drifting Fish Aggregating Devices: a view through the eyes of commercial echosounder buoys. *ICES J. Mar. Sci.* **77**, 2960-2970. (doi:10.1093/icesjms/fsaa178)

Pérez G *et al.* 2020 Effects of habitat modifications on the movement behavior of animals: the case study of Fish Aggregating Devices (FADs) and tropical tunas. *Mov. Ecol.* **8**, 1-11. (doi:10.1186/s40462-020-00230-w)

Rodriguez-Tress P, Capello M, Forget F, Soria M, Beeharry S, Dussooa N, Dagorn L. 2017 Associative behavior of yellowfin Thunnus albacares, skipjack Katsuwonus pelamis, and bigeye tuna T. obesus at anchored fish aggregating devices (FADs) off the coast of Mauritius. *Mar. Ecol. Prog. Ser.* **570**, 213-222. (doi:10.3354/meps12101)

Matsumoto T, Satoh K, Toyonaga M. 2014 Behavior of skipjack tuna (Katsuwonus pelamis) associated with a drifting FAD monitored with ultrasonic transmitters in the equatorial central Pacific Ocean. *Fish. Res.* **157**, 78-85. (doi:10.1016/j.fishres.2014.03.023)

Robert M, Dagorn L, Deneubourg JL, Itano D, Holland K. 2012 Size-dependent behavior of tuna in an array of fish aggregating devices (FADs). *Mar. Biol.* **159**, 907-914. (doi:10.1007/s00227-011-1868-3)

Govinden R, Capello M, Forget F, Filmalter JD, Dagorn L. 2021 Behavior of skipjack (Katsuwonus pelamis), yellowfin (Thunnus albacares), and bigeye (T. obsesus) tunas associated with drifting fish aggregating devices (dFADs) in the Indian Ocean, assessed through acoustic telemetry. *Fish. Oceanogr.* , fog.12536. (doi:10.1111/fog.12536).

Capello M, Deneubourg JL, Robert M, Holland KN, Schaefer KM, Dagorn L. 2016 Population assessment of tropical tuna based on their associative behavior around floating objects. Sci. Rep. 6, 36415. (doi:10.1038/srep36415)

Duparc A et al.. Development status of the new Tropical Tunas Treatment (T3) software. 22nd session of the IOTC Working Party on Tropical Tunas - Data preparatory meeting, 2020, Online, Seychelles. pp.1--5, ⟨10.5281/zenodo.3878125⟩. https://hal.science/hal-03184884

# Supplementary Information

## SI.1. Estimation of the number of floating objects ($\hat{\boldsymbol{p}}$)

The estimation of the number of FOBs in each of the time-area units followed two different approaches. From 2013 to 2019, it was assessed from the number of buoys equipping the DFADs deployed by the French tuna purse seine fleet (nfrench buoys), and two raising factors. The ratio between DFADs deployed by French and Spanish purse-seiners fleets ($R_1$) provided from 2010 to the end of 2017, by Katara et al.[1], allowed estimates of the total number of DFADs. The missing ratios for the 2018 and 2019 were estimated using the average ratio over the year 2017, based on the assumption of a relative stabilization in the exploitation of buoys between the different fleets after this period (limitation measures on the number of buoys operated by tuna purse-seiners in the Indian Ocean: IOTC Resolutions 15/08 and 17/08).

The total number of FOBs in each strata was then derived from the ratios $R_2$ of DFADs encountered by observers on-board French tuna seiners, relative to other floating objects (referred herein as logs). The latter consist of natural (marine mammals, trees, etc.) or artificial (debris from human activities) floating objects found in the open ocean that are not constructed / deployed by tuna fishers.

$$\hat{P}_{[2013-2019]} = n_{french\ buoys}(1 + R_1)(1 + R_2) \tag{1}$$

This ratio was derived from observers' data collected through the Data Collection Framework (Reg 2017/1004 and 2016/1251) funded by both IRD and the European Union since 2005, and OCUP ("Observateur Commun Unique et Permanent"), an industry-funded program coordinated by ORTHONGEL since 2014, with an overall average coverage rate of about 50% over the years 2013 to 2017[2]. The observer data include the date, time, and location of the main activities of the vessel (*e.g.* fishing sets, installation or modification of FOBs, and searching for FOBs). For every activity occurring on a FOB, the type of operation (*e.g.* deployment, removal, and observation of a FOB) and the type of object (DFAD or LOG) are reported.

From 2020 to 2021, the estimation of FOBs number have benefited from the recent availability of buoy data from tuna purse-seine vessels provided by the IOTC Secretariat (IOTC, 2022). This dataset consist of the monthly mean of the number of operational buoys for each 1°×1° cell of the Indian Ocean, used as a proxy for DFAD number. DFAD number were summed over 10° cells and averaged to the quarter-year temporal resolution. FOB numbers were calculated using DFAD number and data recorded by scientific observers onboard French purse seine vessels (2014-2019). Using observers' data, and the methodology developed in Dupaix et al.[3] we calculated a mean monthly ratio ($R_3$):

$$R_3 = \frac{n_{log}}{n_{fad}} \tag{2}$$

---

[1] Katara I *et al.* 2018 Standardisation of yellowfin tuna CPUE for the EU purse seine fleet operating in the Indian Ocean. *20th Sess. Work. Party Trop. Tuna.*

[2] Goujon M, Relot-Stirnemann A, Moëc E, Bach P, Cauquil P, Sabarros P. 2017 Collecting data on board French and Italian tropical tuna purse seiners with common observers: results of ORTHONGEL'S voluntary observer program OCUP (2013-2017) in the Indian ocean. *IOTC-2017-WPDCS-22*.

[3] Dupaix A, Capello M, Lett C, Andrello M, Barrier N, Viennois G, Dagorn L. 2021 Surface habitat modification through industrial tuna fishery practices. *ICES J. Mar. Sci.* **78**, 3075-3088. (doi:10.1093/icesjms/fsab175)

with $n_{log}$ and $n_{FAD}$ the number of log and DFAD observations respectively. The ratio was then used to calculate the number of FOBs per 10° cell which was used to calculate the number of FOBs over 2020-2021 as follows:

$$\hat{P}_{[2020-2021]} = n_{DFAD}(1 + R_3) \quad (3)$$

## SI.2. Estimation of the missing values of species composition in FOB aggregations

Missing species composition values for a given stratum were estimated using their corresponding estimated marginal means (*a.k.a.* least-squares means) in a reference grid[4]. The reference grid consists of the set of all combinations of predictor levels (*i.e*. the time-area strata) and estimated marginal means were the prediction values from the species composition models. We assessed the species composition of sets using a zero-one-inflated Beta regression model, in which the likelihood was fitted with frequentist inference[5]. An equal weight of one were used for all observations, assuming representativeness in each stratum considering the sample size. The proportion of the target species in the set obtained from the sampling programs formed the response variable, while the year, quarter and spatial strata were predictors. All predictors were used to model the mean, variance, zero-inflated and one-inflated components of the model. Model selections were performed on each model component using a Generalized Akaike Information Criterion. Diagnostics of the selected models were checked: the normalized quantile residuals against the fitted values and the case number (*i.e*. index number), together with their kernel density estimate and a normal Q-Q plot (Fig. S1). The prediction error of the mean species composition per stratum were also assessed using a repeated k-fold cross validation (10 folds repeated 100 times) on the zero-one-inflated Beta regression model per species (Fig. S2). In each iteration, we calculated the average species composition estimated and observed. Secondly, we computed the mean bias error, the root mean square error (RMSE) and the mean absolute error (MAE). We also evaluated the goodness of fit with the adjusted coefficient of determination (adj-$R^2$) computed from a simple linear regression observed values against fitted value (Table S1).

[4] Lenth R V. 2016 Least-Squares Means: The R Package lsmeans. *J. Stat. Softw*. **69**. (doi:10.18637/jss.v069.i01)

[5] Rigby R, Stasinopoulos M, Heller G, De Bastiani F. 2019 Distributions for Modelling Location, Scale and Shape: Using GAMLSS in R. *CRC Press*

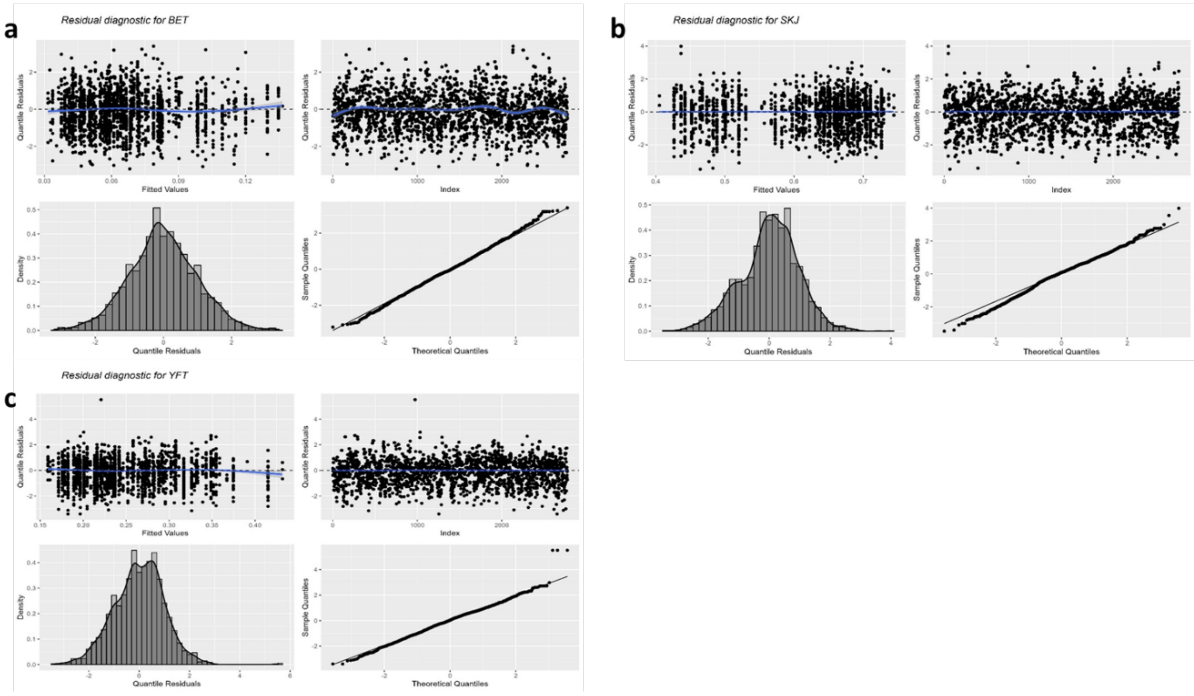


Fig. S1 | Residual diagnostic figures of the zero-one-inflated beta models used to estimate missing mean composition values per strata for (a) bigeye tuna under 10 kg, (b) skipjack, and (c) yellowfin tuna under 10 kg.

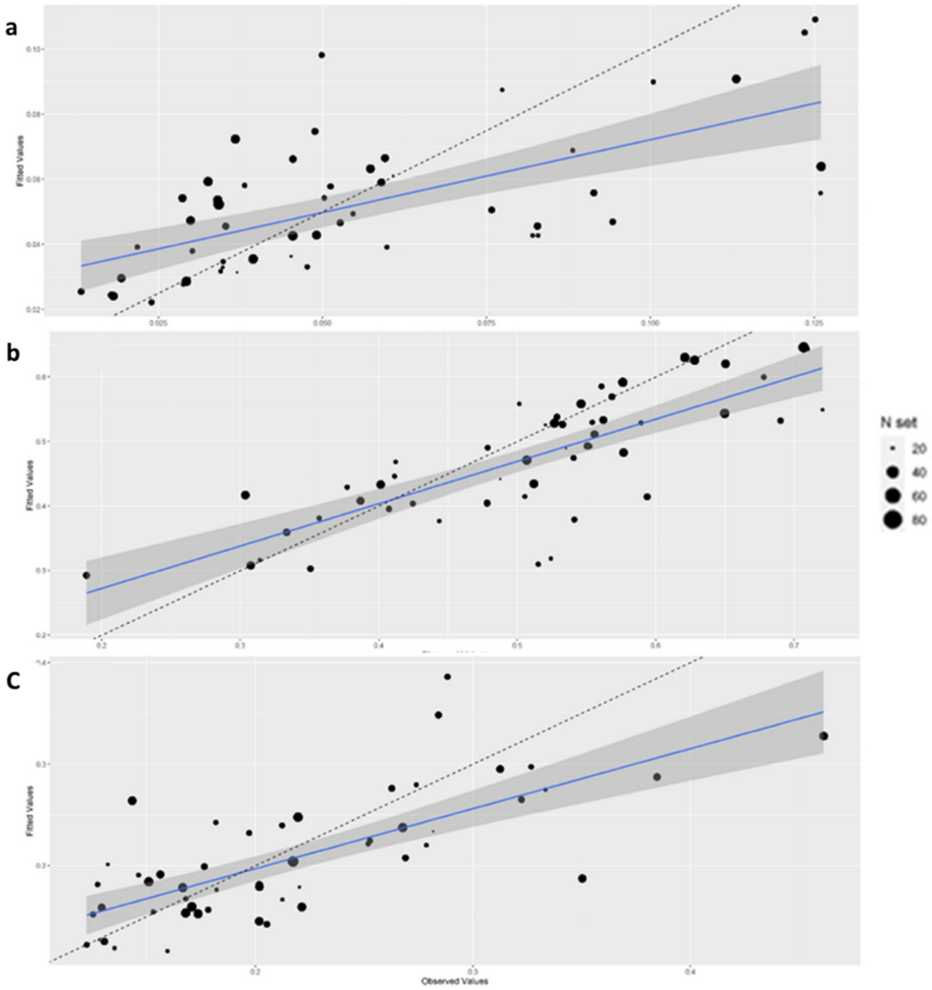


**Fig. S2** | Linear regression of the means proportion per species per strata between fitted value from the zero-one-beta inflated models against observations strata for (a) bigeye tuna under 10 kg, (b) skipjack, and (c) yellowfin tuna under 10 kg. Point size corresponds to the number of sampled sets per strata (N set). Solid line and grey shade correspond to the linear prediction and 95% CI. Dotted line corresponds to the isoline 1:1.

| Species | Bias (mean error) | | Root mean square error (RMSE) | | Mean Absolute Error (MAE) | | cv MAE | | Adjusted coefficient of determination (Adj. $R^2$) | |
|---|---|---|---|---|---|---|---|---|---|---|
| YFT | -0.009 | [-0.0092; -0.0088] | 0.0525 | [0.0523; 0.0528] | 0.0403 | [0.0401; 0.0405] | 0.1876 | [0.1867; 0.1885] | 0.5211 | [0.5175; 0.5243] |
| BET | -0.0032 | [-0.0033; -0.0031] | 0.0234 | [0.0233; 0.0235] | 0.0171 | [0.0170; 0.0172] | 0.3088 | [0.3075; 0.3101] | 0.4096 | [0.4064; 0.4130] |
| SKJ | -0.0344 | [-0.0347; -0.0340] | 0.0788 | [0.0783; 0.0793] | 0.0578 | [0.0575; 0.0583] | 0.1134 | [0.1128; 0.1143] | 0.6139 | [0.6090; 0.6185] |

**Table S1** | Predictive performance indices of the zero-one-beta inflated models per species. Mean and quantiles (0.025; 0.975) were computed from 100 repetitions of 10-fold cross validation. BET: bigeye tuna, SKJ: skipjack tuna, YFT: yellowfin tuna.

## SI.3. Estimation of the missing values of species occurrence in FOB aggregations

Missing occurrence values for a given stratum were estimated from a binomial model using year, quarter and spatial strata as predictors (Fig. S3).

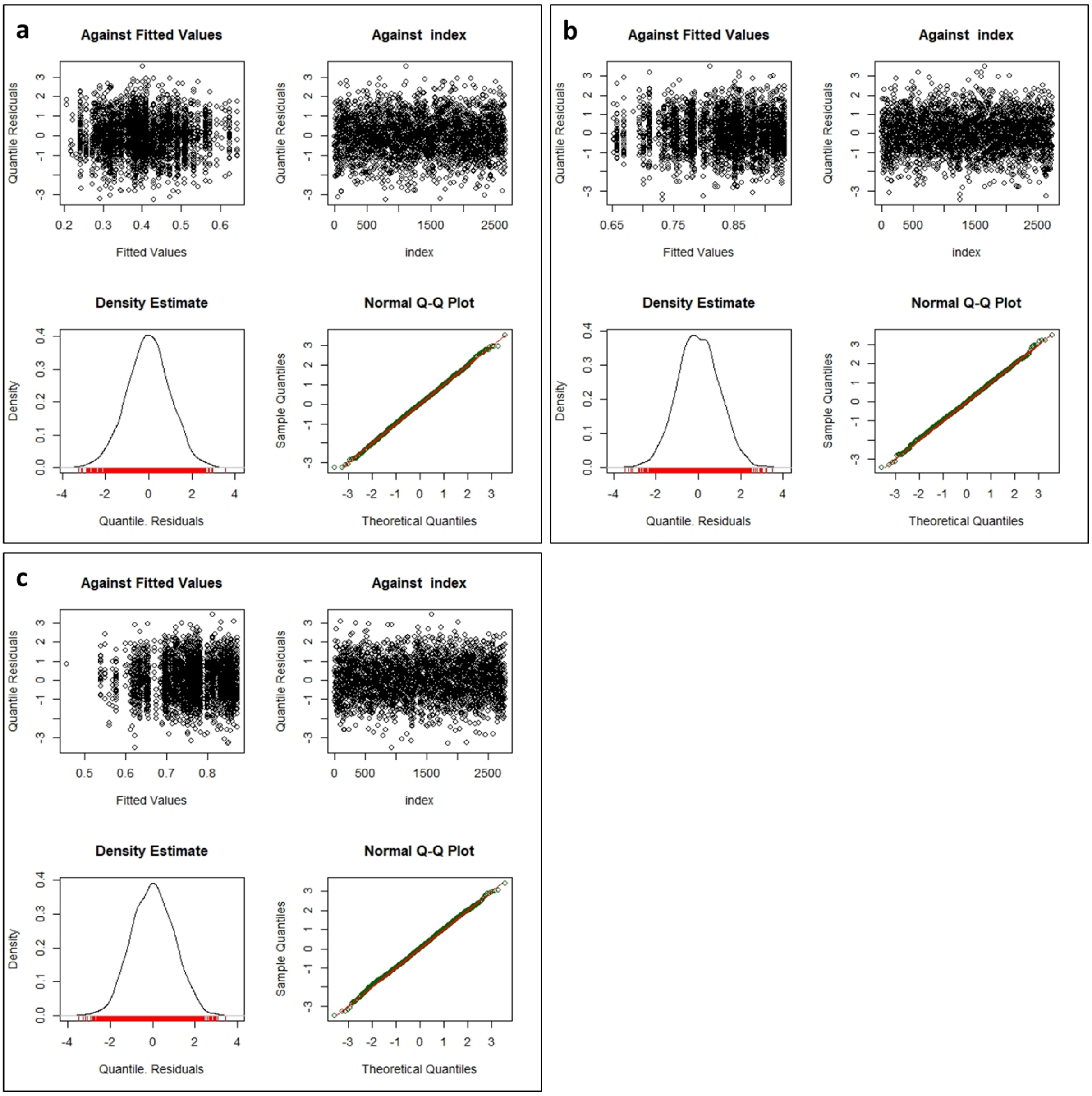


**Fig. S3 |** Residual diagnostic figures of the binomial model used to estimate missing occurrence values (**a**) bigeye tuna under 10 kg, (**b**) skipjack, and (**c**) yellowfin tuna under 10 kg.